Research Article

Effect of Nd^{3+} substitution on structural, ferroelectric, magnetic and electrical properties of $BiFeO_3$–$PbTiO_3$ binary system

Naveen Kumar[1,4] · Bastola Narayan[2] · Manoj Kumar[1] · Arun Kumar Singh[3] · Shobhna Dhiman[1] · Sanjeev Kumar[1]

Abstract
In this paper, we have reported the effect of rare earth Nd^{3+} ion substitution on crystal structure, ferroelectric, electrical and magnetic behavior of morphotropic phase boundary (MPB) composition of polycrystalline ceramics $0.7Bi_{(1-x)}Nd_xFeO_3$–$0.3PbTiO_3$(BNFPT), where x = 0, 0.05, 0.10. Rietveld refinement of XRD profiles confirms coexistence of rhombohedral*R3c* and tetragonal *P4mm*polymorphs forming MPB for all the compositions. We observed that the remnant polarization P_r increases with increasing Nd^{3+} concentration. Piezoelectric studies show gradual increase in piezoelectric coefficient (d_{33}) from 11 to 34 pC/N with increase in Nd^{3+} concentration for BNFPT samples. All compositions exhibit weak ferromagnetic character. For the same composition range, the study of dielectric behavior revealed gradual decrease in Curie temperature (T_c) as we increased doping content of Nd^{3+}.

Keywords Rietveld refinement · Magnetization · MPB · Piezoelectric · $BiFeO_3$–$PbTiO_3$

1 Introduction

Multiferroic materials with ferroelectric, ferromagnetic and ferroelastic properties represent a promising and appealing class of smart materials [1, 2]. These materials have attracted numerous research activities due to their potential applications as multifunctional devices [3]. Perovskite-type $BiFeO_3$ (BFO) is one of the most extensively studied multiferroic material which attains $a^-a^-a^-$ tilted octahedral structure [4] and crystallizes to distorted rhombohedral phase with R3c space group and unit cell parameter: $a = 5.58$ Å and $c = 13.9$ Å [5, 6]. BFO possesses both antiferromagnetic ($T_N \sim 643$ K) and ferroelectric ($T_c \sim 1143$ K) ordering much above the room temperature [7, 8]. Beside this, BFO has some inherent tribulations: formation of secondary phases, high leakage current and lack of structural distortion. Low spontaneous saturation magnetization is also one of the drawback which is due to spin helical ordering of magnetic moments that suppresses magneto-electric coupling between ordered parameters i.e. ferroelectricity and magnetism [5, 6]. Low resistivity of bulk BFO samples makes it difficult to display well saturated ferroelectric P–E loops [5]. The reason of low resistivity of the BFO sample is mainly because of different oxidation states of Fe ions i.e. $Fe^{3+/2+}$ and also due to anion vacancies, which not only affect the ferroelectric properties but also have a detrimental effect on magnetic properties [9, 10]. In order to overcome these limitations and also to enhance ferroelectric and ferromagnetic properties several reports are available on substitution of rare earth materials La^{3+}, Eu^{3+}, Pr^{3+}, Gd^{3+} and Nd^{3+} [11–15] on A-site of BFO. The substitution of smaller magnetic rare earth cation Nd^{3+} for larger Bi^{3+} in bulk BFO and thin films have modulated the structural parameters thereby destroying spin cycloid which further results in weak ferromagnetism [16, 17]. Gaur et al. have also reported the reduction in

✉ Sanjeev Kumar, sanjeev04101977@gmail.com | [1]Applied Sciences Department, Punjab Engineering College (Deemed to be University), Chandigarh 160012, India. [2]Department of Materials Engineering, Indian Institute of Science, Bengaluru 560012, India. [3]Electronics and Communications Engineering Department, Punjab Engineering College (Deemed to be University), Chandigarh 160012, India. [4]Deparment of Physics, G.G.D.S.D College, Chandigarh 160032, India.

SN Applied Sciences (2019) 1:874 | https://doi.org/10.1007/s42452-019-0919-0

Received: 13 May 2019 / Accepted: 11 July 2019 / Published online: 19 July 2019

leakage current and absence of secondary phases by Nd^{3+} substitution in BFO [15]. Lin et al. studied the Nd_2O_3 modified tetragonal $BaTiO_3$/PVDF ceramic composites for high performance capacitors [18] and the same group also investigated the Nd-$BaTiO_3$/PVDF ceramic/polymer composite for capacitor applications [19].

Another way to enhance the properties of BFO, is by making binary solution with other perovskites such as $CaTiO_3$, $BaTiO_3$, $PbTiO_3$ and $SrTiO_3$ [20–23] have also been reported. Despite all, $(1-x)BiFeO_3$–$xPbTiO_3$(BF–PT)solid solutions show interesting properties such as high tetragonality, high Curie temperature and morphotropic phase boundary (MPB) [24–26]. BF–PT binary system exhibits morphotropic phase boundary at x = 0.3 with a coexistence of rhombohedral (R3c) and tetragonal (P4mm) polymorphs [27]. BF–PT ceramic samples have gathered tremendous interest among researchers due to enhanced multiferroic character [28]. Cotica et al. reported the control over crystalline phase and ferroelectric behavior by La substitution in 0.6BF–0.4PT [29]. Mohanty et al. have found improved dielectric and ferroelectric properties of Dy^{3+} substituted 0.5BF–0.5PT composites by doping of Dy^{3+} ions [30]. Recently, Sahu et al. have reported enhanced resistivity and relaxor dielectric behavior above room temperature in Gd^{3+} modified 0.8BF–0.2PT ceramic samples [31]. The same group also reported the enhancement in dielectric behavior with increase in Sm^{3+} doping in 0.8BF–0.2PT solid solutions [32].

The structural, dielectric, ferroelectric and ferromagnetic properties of BFO and BF–PT ceramics has been clearly affected by rare earth element substitution, as discussed above. The oxygen anions, which lie very close to Bi-site in the unit cell of BFO, are unstable due to volatile character of Bi. Therefore, Nd^{3+} substitution on Bi-site can play extensive role in the improvement of structural, ferroelectric, magnetic and electrical properties of multiferroics [33], this motivated us to investigate the effect of Nd^{3+} substitution in BF–PT multiferroic binary system.

2 Experimental

Polycrystalline ceramic samples of $0.7Bi_{(1-x)}Nd_xFeO_3$–0.3PbTiO$_3$ (x = 0, 0.05, 0.10) were synthesized by conventional oxide mixing route. Initially, stoichiometric amounts of analytical grade high purity oxides Bi_2O_3, Nd_2O_3, Fe_2O_3, PbO and TiO_2 (Sigma Aldrich) were mixed together and thoroughly grounded for 12 h in the presence of acetone (which acts like a mixing media) in a planetary ball mill (P5, Fritch). Then powders were calcined at 820 °C for 2 h in air. After the process of calcination, the samples were mixed with PVA (2 wt%), compressed into small cylindrical discs (2 mm thick and 12 mm in diameter) under pressure of 50 MPa using a hydraulic press. These pellets were sintered at 900–950 °C for 2 h in air. To avoid the volatilization of Bi and Pb, the powder of the same composition as a spacer was surrounded all around the pellets and the pellets were covered with an alumina cup and sealed with MgO. The pellets of high density were further being used for characterization.

One of the pellet of each composition (x = 0, 0.05 and 0.10) was grounded and annealed at 700 °C for 1 h to release the stresses produced at the time of sintering. The annealed powder was used for phase analysis using Cu Kα radiation in X-ray diffractometer (Rigaku, Japan) within a scanning angle range $10° \le 2\theta \le 90°$. The pellets were polished up to the thickness of ~0.7 mm and both faces of the pellets were silver electroded. The ferroelectric hysteresis loops (P–E loops) were measured using P–E loop tracer (Precision Premier II loop tracer, Radiant). High temperature dielectric characterization was done using impedance analyzer (Novocontrol, Alpha AN). The magnetic properties of the compositions were studied using vibrating sample magnetometer (LakeShore). The piezoelectric coefficients of the samples were recorded using piezo-meter (Berlincourt Piezotest PM 300).

3 Results and discussion

Crystallinity of $0.7Bi_{(1-x)}Nd_xFeO_3$–$0.3PbTiO_3$ (x = 0, 0.05, 0.10) ceramic compositions was examined using X-ray diffraction (XRD) profiles with a scanning rate of 1°/min within angle range $10° \le 2\theta \le 90°$. The crystal structure of BFO is rhombohedral with space group *R3c* [5] and $NdFeO_3$ is orthorhombic with space group *Pbnm* [34], whereas like $BaTiO_3$, $PbTiO_3$ exhibits tetragonal symmetry with space group *P4mm* [35]. The crystal stability of ABO_3-type perovskites is generally elaborated in terms of Goldschmidt tolerance factor 't'. The tolerance factor 't' can be expressed as an equation given below:

$$t = \frac{\left[0.7(1-x)R_{Bi^{3+}} + xR_{Nd^{3+}} 0.3R_{Pb^{2+}} + R_{O^{2-}}\right]}{\sqrt{2}\left[0.7R_{Fe^{3+}} + 0.3R_{Ti^{4+}} + R_{O^{2-}}\right]} \quad (1)$$

The tolerance factor 't' is found to be 0.8913, 0.8907 and 0.8903 for x = 0, x = 0.05 and x = 0.10, respectively. The structural stability merely decreases upon increasing Nd^{3+} content in the compositions. To confirm the exact crystalline phase of as-synthesized compositions, Rietveld refinement method has been employed using FULLPROF software [36]. The two phase model (i.e. rhombohedral *R3c* and tetragonal *P4mm*) approach has been adopted for Rietveld refinement measurements. Figure 1 shows the refined XRD profiles of all the samples, which also indicates that all the compositions exhibit pure perovskite crystallinity with no secondary phases or traces of

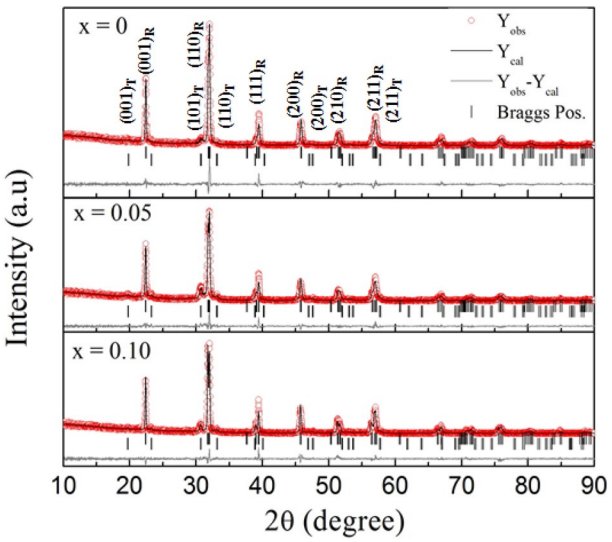

Fig. 1 Rietveld refined XRD diffraction patterns of $0.7Bi_{(1-x)}Nd_xFeO_3$–$0.3PbTiO_3$ (x = 0, 0.05, 0.10)

pyrochlore. The refinement calculations for all the three compositions x = 0, 0.05 and 0.10, illustrate the existence of morphotropic phase boundary between polymorphs of rhombohedral and tetragonal symmetries. The refinement results are in well agreement with the earlier reports published on MPB compositions of BF–PT binary system [26]. The lattice parameters a_R, c_R of rhombohedral unit cell and a_T, c_T of tetragonal unit cell are determined through refinement calculations. Figure 2a, b displays the effect of Nd^{3+}substitution in BFO lattice framework, due to which unit cell lattice parameters of rhombohedral and tetragonal phase changes. The data obtained from Rietveld refinement studies has been used for bond angles and bond lengths calculations. The statistical parameter (R-factors), goodness of fit value (χ^2), bond angles and bond lengths are given in Table 1. The variations in bond lengths and bond angles clearly indicate that there exists substantial effect of Nd^{3+} intrusion at Bi^{3+} site.

3.1 Ferroelectric studies

Figure 3 represents polarization versus electric field plots for $0.7Bi_{(1-x)}Nd_xFeO_3$–$0.3PbTiO_3$ (x = 0, 0.05, 0.10), measured at a frequency of 50 Hz at room temperature. As BFO, shows very weak ferroelectric response because of low value of resistivity ($\rho \sim 10^6$ Ω cm) [6]. The conductive behavior of BFO restricts the application of higher field limits the ferroelectric behavior [5].The leakage current observed in $NdFeO_3$–$PbTiO_3$ system is less than that of $BiFeO_3$–$PbTiO_3$ binary system, which is mainly due to lanthanide ion (Nd^{3+}) [37]. The coercive field E_c and remnant polarization P_r increases with increasing Nd^{3+} content. The observed value of remnant polarization for x = 0, 0.05 and 0.10 is 3.4 μC/cm^2, 5.6 μC/cm^2 and 6.0 μC/cm^2, respectively. Kim et al. have also observed the similar ferroelectric phenomenon in rare earth ion (Pr) modified $BiFeO_3$–$PbTiO_3$ solid solution [38]. XRD studies confirm the variation in lattice parameter with Nd^{3+} intrusion in the BFO matrix, which also distorts the tetragonal unit cell at MPB region. The distortion in tetragonal unit cell leads to the hybridization in O(2*p*) and Ti(3*d*) orbital, which induces the effective polarization in the crystal. It is reported that domain switching will be easy due to 8 polar directions along [111] in rhombohedral phase and 6 polarization directions of tetragonal structure are along [001], which lead to easy crystal orientations [39]. Conventionally, ferroelectric distortion in insulating perovskites is stabilized due to transfer of electric charge of oxygen anion to neighboring unoccupied d-orbital of transition metal. Due to partial substitution of Nd^{3+} ion at Bi^{3+} site in the BFO matrix, a $6s^2$ lone pair of Bi^{3+} hybridize with vacant 2p orbital of oxygen anion to produce a local lobe, thereby constructing non-centrosymmetric distortion in x = 0.05 and x = 0.10 [40] and hence induces ferroelectricity in the system.

3.2 Magnetic studies

The plots of magnetization (M) as a function of applied magnetic field (H) for x = 0, 0.05 and 0.10 ceramics are shown in Fig. 4. It is well known that rhombohedrally distorted BFO crystal exhibits G-type antiferromagnetism and $PbTiO_3$ shows diamagnetic character similar to $BaTiO_3$ [41]. It is clear from the Fig. 4 that magnetic hysteresis is not completely antiferromagnetic but it exhibits weak ferromagnetic behavior with small remnant magnetization. The value of remnant magnetization M_r for x = 0, 0.05 and 0.10 is found to be 5.3 memu/g, 8.3 memu/g and 15.2 memu/g, respectively. The similar phenomenon has also been observed by Freitas et al. for $0.6BiFeO_3$–$0.4PbTiO_3$ composition, where chemically arranged magnetic clusters attribute to small remnant magnetization in the ceramic system [42]. Nd^{3+} substitution in $BiFeO_3$ crystal lattice disturbs the spiral magnetic spin wave and hence induces ferromagnetism in the system, which also correlates with XRD pattern, where $(104)_R$ peak intensity variation of rhombohedral unit cell can be clearly seen in Fig. 1. Indeed, it also has been illustrated that structural transformation occurs form rhombohedral to triclinic crystalline phase, which give rise to continuous collapse in spin cycloid [43, 44]. Also Ti^{4+} ions of $PbTiO_3$ compound dilutes the Fe^{3+}cations super-exchange mechanism i.e. Fe^{3+}–O–Ti^{4+}–O–Fe^{3+} occurs between two neighboring Fe ions. This long range bond order deteriorates Fe^{3+}–O–Fe^{3+} bond with a sudden collapse in modulated spin wave and consequently releases magnetization in ordered magnetic micro-regions.

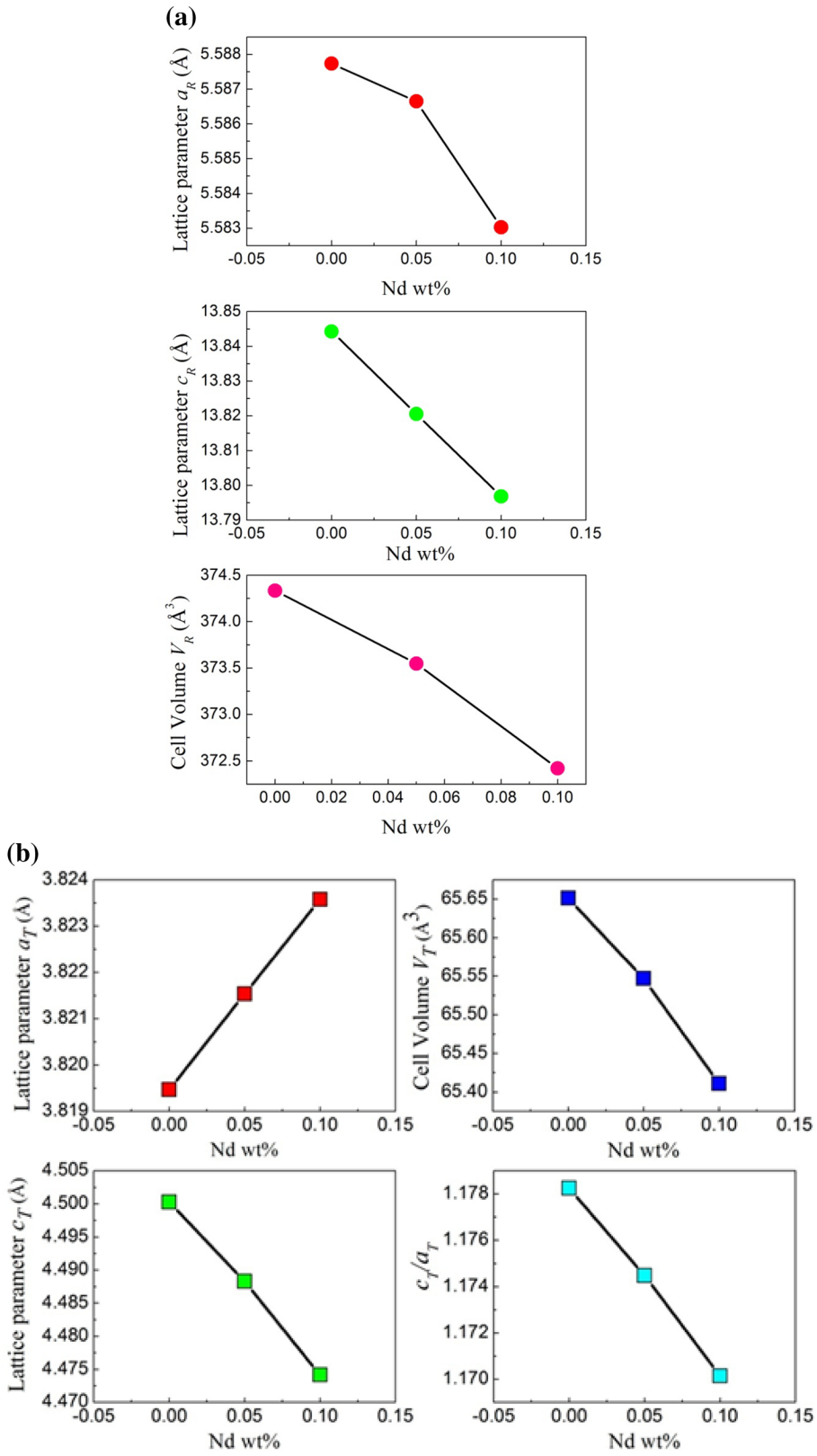

Fig. 2 **a** Lattice parameter and unit cell volume of rhombohedral R3c phase as a function of Nd^{3+} wt%. **b** Lattice parameter, unit cell volume, strain ratio ($\frac{c_T}{a_T}$) of tetragonal P4mm phase as a function of Nd^{3+} wt%

Table 1 Statistical parameter, lattice parameter, bond angles and bond lengths of $0.7Bi_{(1-x)}Nd_xFeO_3$–$0.3PbTiO_3$ (x = 0, 0.05, 0.10)

Composition	Lattice parameter (Å)			Cell volume (Å^3)	Bond lengths (R3c)		Bond angles (R3c)	
	a	*b*	*c*					
x = 0 Rhombohedral (R-R3c)	5.587736	5.587736	13.84429	374.334	Bi-O3	2.40787	O–Bi–O	92.858
							O–Fe–O	116.186
					Fe–O3	1.61086	Bi–O–Fe	101.910
Tetragonal (T-P4mm)	3.819469	3.819469	4.500269	65.6514	R: R_{Bragg} = 5.98; R_F = 4.16 T: R_{Bragg} = 19.2; R_F = 14.0 χ^2 = 1.53			
x = 0.05 Rhombohedral (R-R3c)	5.586649	5.586649	13.82055	373.547	Bi–O3	2.45783	O–Bi–O	91.502
							O–Fe–O	115.623
					Fe–O3	1.60237	Bi–O–Fe	103.134
Tetragonal (T-P4mm)	3.821537	3.821537	4.488287	65.547	R: R_{Bragg} = 4.63; R_F = 2.92 T: R_{Bragg} = 10.2; R_F = 7.08 χ^2 = 1.68			
x = 0.10 Rhombohedral (R-R3c)	5.583030	5.583030	13.79680	372.422	Bi–O3	2.5646	O–Bi–O	92.677
							O–Fe–O	115.482
					Fe–O3	1.7099	Bi–O–Fe	101.192
Tetragonal (T-P4mm)	3.823580	3.823580	4.474155	65.4 11	R: R_{Bragg} = 6.37; R_F = 3.61 T: R_{Bragg} = 22.3; R_F = 15.1 χ^2 = 1.82			

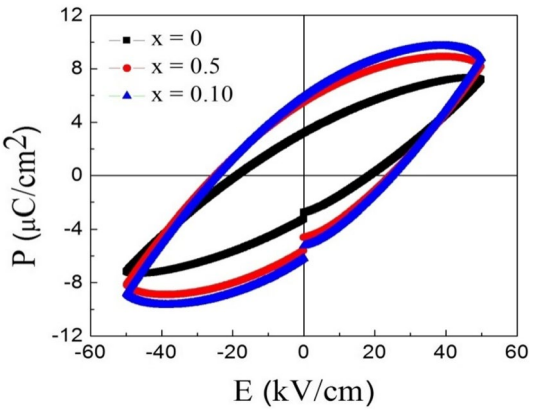

Fig. 3 P–E loops of $0.7Bi_{(1-x)}Nd_xFeO_3$–$0.3PbTiO_3$ (x = 0, 0.05, 0.10)

3.3 Dielectric studies

Figure 5 illustrates the real part of dielectric constant (ε′) and loss tangent (tanδ) as a function of temperature (T) measured at 10 kHz for x = 0, 0.05 and 0.10. For ferroelectric to paraelectric phase transition, there exists a peak in dielectric graph, which corresponds to structural transition temperature or Curie temperature (T_c). The low value of dielectric permittivity at room temperature is mainly because of semiconducting nature of BFO. As the value of temperature increases, dipole ordering increases as well as the dielectric constant. Nd^{3+} doping reduces the dielectric loss thereby increasing the resistivity of the sample [45]. In addition, Nd^{3+} substitution also prevents the Bi-volatility and reduces the oxygen anion vacancies [39]. As published in earlier reports that rare-earth substitution in BF–PT binary system lowers down the value of Curie temperature T_c [44]. The high value of transition temperature in this system is because of strong correlation amongst A-site (Bi^{3+}/Pb^{2+}), B-site (Ti^{4+}/Fe^{3+}) cations and also due to high value of tetragonal strain ($\frac{C_T}{a_T}$). Nd^{3+} substitution thereby reduces the coupling between the cations and hence reduces the tetragonal strain. A dielectric anomaly observed below 300 °C may be attributed due to interaction between Fe^{3+}/Fe^{2+} ions and oxygen anions through redox reaction [46]. The decrease in transition temperature by adding Nd^{3+} attributes to softening of repulsive force of short range against the ferroelectric ordering [47]. Similar phenomenon have also been observed in Sm doped BFO [48]. Therefore, the value of transition temperature decreases with increasing Nd^{3+} concentration. Curie temperature is found to be 477 °C, 476 °C and 450 °C for x = 0, 0.05 and 0.10, respectively. Similar trend has been observed in rare earth Dy^{3+} and La^{3+} doped BF–PT ceramics, where transition temperature decreases with increasing rare earth concentration in the BF–PT system [30, 40, 49].

3.4 Piezoelectric studies

The piezoelectric coefficients of x = 0, 0.05 and 0.10 ceramic compositions were measured using Berlincourt peizo-meter. The value of piezoelectric coefficient

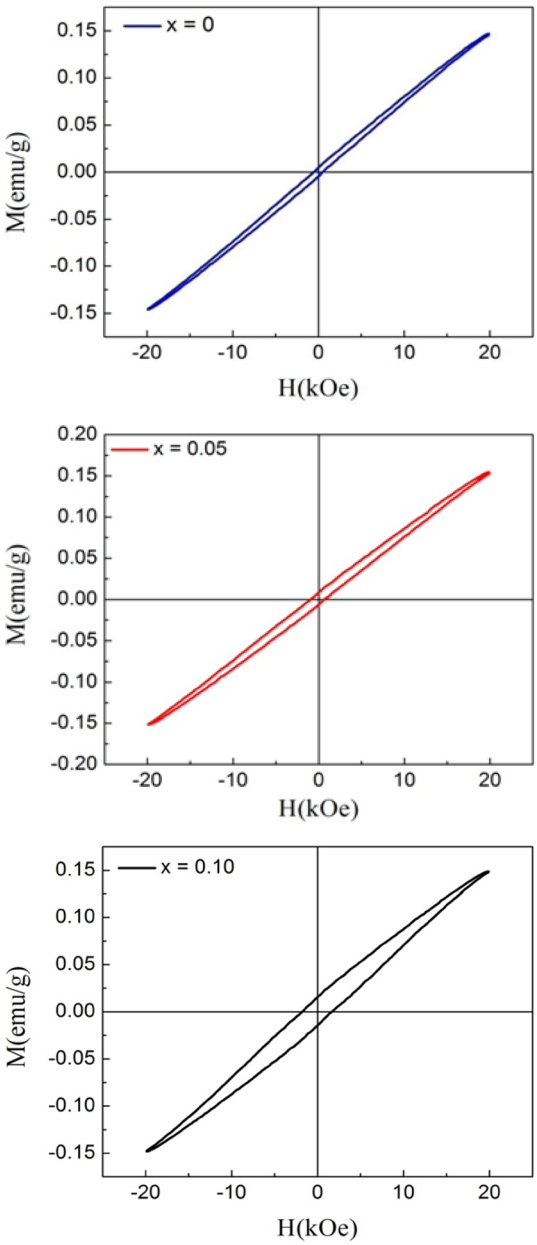

Fig. 4 M–H loops of $0.7Bi_{(1-x)}Nd_xFeO_3$–$0.3PbTiO_3$ (x = 0, 0.05, 0.10)

increases with increasing Nd^{3+} concentration in BF–PT. The piezoelectric coefficients are 11 pC/N, 18 pC/N and 34 pC/N for x = 0, 0.05 and 0.10, respectively. It indicates that piezoelectric response enhances due to Nd^{3+} and also due to multiphase coexistence region (i.e. MPB region). The piezoelectric results are in agreement with the fact that reduction in tetragonal strain $\frac{C_T}{a_T} \sim 1.17–1.14$, enhances the probability of hybridization between d-orbital of transition metal (Fe/Ti) and p-orbital of oxygen anion in perovskites. Jiang also reported that Nd^{3+} substitution in BFO enhances the piezoelectric properties [50].

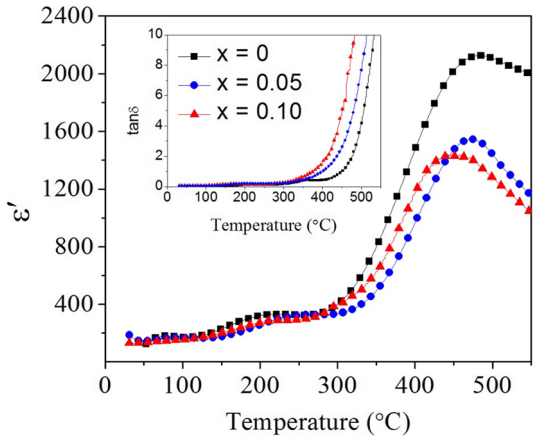

Fig. 5 Real part of dielectric constant (ε′) and loss tangent (tanδ) as a function temperature for $0.7Bi_{(1-x)}Nd_xFeO_3$–$0.3PbTiO_3$ (x = 0, 0.05, 0.10)

4 Conclusions

Polycrystalline ceramic samples $0.7Bi_{(1-x)}Nd_xFeO_3$–$0.3PbTiO_3$ (x = 0, 0.05, 0.10) were successfully synthesized with purely perovskite crystallinity by standard solid state reaction method. Room temperature XRD, ferroelectric and magnetic properties were investigated to illustrate the effect of A-site substitution on crystalline phase and multiferroic properties for x = 0.10 perovskite demonstrating enhanced ferroelectric and canted ferromagnetic behavior. A variation in dominant antiferromagnetic behavior was observed within the composition range i.e. x = 0–0.10, where antiferromagnetism to weak ferromagnetic transition takes place. It has been observed that Nd^{3+} substitution enhanced the polar ionic displacement and resulted in improved ferroelectric characteristic of the ceramic sample as value of remnant polarization increased from 3.4 to 6.0 μC/cm^2 from x = 0 to 0.10, respectively. The dielectric measurements revealed that transition temperature of the composition decreases with increasing isovalent Nd^{3+} ion concentration. Nd^{3+} doped multiphase $0.7BiFeO_3$–$0.3PbTiO_3$ ceramic composition with improved multiferroic properties makes the material very promising candidate for potential applications.

Acknowledgement Sanjeev Kumar is thankful to Punjab Engineering College (Deemed to be University), Chandigarh for providing financial assistance in the form of RIPA Project. He is also thankful to Prof. Rajeev Ranjan for providing the research facilities available in his lab. Naveen Kumar is thankful to Punjab Engineering College (Deemed to be University), for providing fellowship. He is also thankful to NRC-M (Materials Engineering, IISc, Bengaluru) for carrying out characterization work.

Compliance with ethical standards

Conflict of interest On behalf of all authors, the corresponding author states that there is no conflict of interest.

References

1. Schmid H (1994) Multi-ferroic magnetoelectrics. Ferroelectrics 162:317–338
2. Fiebig M (2005) Revival of the magnetoelectric effect. J Phys D 38:R123–R152
3. Eerenstein W, Mathur ND, Scott JF (2006) Multiferroic and magnetoelectric materials. Nat Rev 442:759–765
4. Glazer AM (1975) Simple ways of determining perovskite structures. Acta Crystallogr Sec A 31:756–762
5. Catalan G, Scott JF (2009) Physics and applications of bismuth ferrite. Adv Mater 21:2463–2485
6. Kubel F, Schmid H (1990) Structure of a ferroelectric and ferroelastic monodomain crystal of the perovskite $BiFeO_3$. Acta Crystallogr B 46:698–702
7. Kumar MM, Palkar VR, Srinivas K, Suryanarayan SV (2000) Ferroelectricity in a pure $BiFeO_3$ ceramic. Appl Phys Lett 76:2764–2768
8. Wang YP, Zhou Zhang MF, Chen XY, Liu JM, Liu ZG (2004) Room-temperature saturated ferroelectric polarization in $BiFeO_3$ ceramics synthesized by rapid liquid phase sintering. Appl Phys Lett 84:1731–1733
9. Cheng JR et al (2003) Structural and dielectric properties of Ga-modified $BiFeO_3$–$PbTiO_3$ crystalline solutions. J Appl Phys 94:5153–5157
10. Eerenstein W, Morrison FD, Dho J, Blamire MG, Scott JF, Mathur ND (2005) Comment on" Epitaxial $BiFeO_3$ multiferroic thin film heterostructures". Science 307:1203a
11. Das SR, Choudhary RNP, Bhattacharya P, Katiyar RS (2007) Structural and multiferroic properties of La-modified $BiFeO_3$ ceramics. J Appl Phys 101:034104-7
12. Chakrabarti K, Das K, Sarkar B, Ghosh S, De SK, Sinha G, Lahtinen J (2012) Enhanced magnetic and dielectric properties of Eu and Co co-doped $BiFeO_3$ nanoparticles. Appl Phys Lett 101:042401-3
13. Yu B, Li M, Hu Z, Pei L, Guo D, Zhao X, Dong S (2008) Enhanced multiferroic properties of the high-valence Pr doped $BiFeO_3$ thin film. Appl Phys Lett 93:182909-3
14. Khomchenko VA, Kiselev DA, Bdikin IK, Shvartsman VV, Borisov P, Kleemann W, Vieira JM, Kholkin AL (2008) Crystal structure and multiferroic properties of Gd-substituted $BiFeO_3$. Appl Phys Lett 93:262905-3
15. Gaur A, Singh P, Choudhary N, Kumar D, Shariq M, Singh K, Kaur N, Kaur D (2011) Structural, optical and magnetic properties of Nd-doped $BiFeO_3$ thin films prepared by pulsed laser deposition. Phys B Condensed Matter 406:1877–1882
16. Yuan GL, Or SW, Liu JM, Liu ZJ (2006) Structural transformation and ferroelectromagnetic behavior in $Bi_{1-x}Nd_xO_3$ single-phase multiferroic ceramics. Appl Phys Lett 89:052905-3
17. Huang FZ, Hu X, Lin W, Wu X, Kan Y, Zhu J (2006) Effect of Nd dopant on magnetic and electric properties of $BiFeO_3$ thin films prepared by metal organic deposition method. Appl Phys Lett 89:242914-3
18. Lin MF, Thakur VK, Tan EJ, Lee PS (2011) Dopant induced hollow $BaTiO_3$ nanostructures for application in high performance capacitors. J Mater Chem 21:16500–16504
19. Lin MF, Lee PS (2013) Formation of PVDF-g-HEMA/$BaTiO_3$ nanocomposites via in situ nanoparticle synthesis for high performance capacitor applications. J Mater Chem A 1:4614455–4614459
20. Wang QQ, Wang Z, Liu Xand Chen XM (2012) Improved structure stability and multiferroic characteristics in $CaTiO_3$–modified $BiFeO_3$ ceramics. J Am Ceram Soc 95:670–675
21. Kumar MM, Srinath S, Kumar GS, Suryanarayana SV (1998) Spontaneous magnetic moment in $BiFeO_3$–$BaTiO_3$ solid solutions at low temperatures. J Magn Mag Mat 188:203–212
22. Zhu WM, Guo HY, Ye ZG (2008) Structural and magnetic characterization of multiferroic $(BiFeO_3)_{1-x}(PbTiO_3)_x$ solid solutions. Phys Rev B 78:014401(1–10)
23. Liu H, Yang X (2016) Structural, dielectric, and magnetic properties of $BiFeO_3$–$SrTiO_3$ solid solution ceramics. Ferroelectrics 500:310–317
24. Fedulov SA, Ladyzhinskii PB, Pyatigorskaya IL, Venevetsev YN (1964) Complete phase diagram of the $PbTiO_3$–$BiFeO_3$ system. Soviet Phys Solid State 6:375
25. Smith RT, Achenbach GD, Gerson R, James WJ (1968) Dielectric properties of solid solutions of $BiFeO_3$ with Pb(Ti, Zr)O_3 at high temperature and high frequency. J Appl Phys 39:70–74
26. Sai Sunder VVS, Halliyal A, Umarji AM (1995) Investigation of tetragonal distortion in the $PbTiO_3$–$BiFeO_3$ system by high-temperature X-ray diffraction. J Mater Res 10:1301–1306
27. Comyn TP, Stevenson T, Al-Jawad M, André G, Bell AJ, Cywinski R (2011) Antiferromagnetic order in tetragonal bismuth ferrite–lead titanate. J Magn Magn Mater 323:3232533–3232538
28. Bennett J, Shrout TR, Zhang SJ, Mandal P, Bell AJ, Stevenson TJ, Comyn TP (2014) Temperature dependence of the intrinsic and extrinsic contributions in $BiFeO_3$–$(K_{0.5}Bi_{0.5})TiO_3$–$PbTiO_3$ piezoelectric ceramics. J Appl Phys 116:094102-9
29. Cotica LF, Estrada FR, Frutitas VF, Dias GS, Santos IA, Eiras JA, Garcia D (2011) Ferroic states in La doped $BiFeO_3$–$PbTiO_3$ multiferroic compounds. J Appl Phys 111:114105–114110
30. Mohanty NK, Behera AK, Satpathy SK, Behera B, Nayak P (2015) Effect of dysprosium substitution on structural and dielectric properties of $BiFeO_3$–$PbTiO_3$ multiferroic composites. J Rare Earths 33:639–646
31. Sahu T, Patra AK, Behera B (2017) Effect of Gadolinium doping on structural, ferroic and electrical properties of $0.8BiGd_xFe_{1-x}O_3$–$0.2PbTiO_x$ (x = 0.00, 0.05, 0.10, 0.15 and 0.20) composites. J Alloys Compd 695:2273–2284
32. Sahu T, Behera B (2017) Investigation on structural, dielectric and ferroelectric properties of samarium-substituted $BiFeO_3$–$PbTiO_3$ composites. J Adv Dielectr 7:1750001-6
33. Singh MK, Jang HM, Gupta HC, Katiyar RS (2008) Polarized Raman scattering and lattice eigen modes of antiferromagnetic $NdFeO_3$. J Raman Spectrosc 39:842–848
34. Yuan SJ, Ren W, Hong F, Wang YB, Zhang JC, Bellaiche L, Cao SX, Cao G (2013) Spin switching and magnetization reversal in single-crystal $NdFeO_3$. Phy Rev B 87:184405
35. Lin MF, Thakur VK, Tan EJ, Lee PS (2011) Surface functionalization of $BaTiO_3$ nanoparticles and improved electrical properties of $BaTiO_3$/polyvinylidene fluoride composite. RSC Adv 1:576–578
36. Rodriguez-Carvajal J (2007) Laboratory, FULLPROF, a Rietveld and pattern matching analysis program. Laboratoire Leon Brillouin, CEA-CNRS, France
37. Kumar S, Pal J, Kaur S, Sharma V, Dahiya S, Bahu PD, Singh M, Ray A, Maitra T, Singh A (2018) Correlation between multiferroic properties and processing parameters in $NdFeO_3$–$PbTiO_3$ solid solutions. J Alloys Compd 764:824–833
38. Kim JS, Cheon CI, Choi YM (2003) Ferroelectric and ferromagnetic properties of $BiFeO_3$–$PrFeO_3$–$PbTiO_3$ solid solutions. J Appl Phys 93:9263–9270
39. Pang D, He C, Long X (2017) Multiferroic ternary solid solution system of $BiFeO_3$–$NdFeO_3$–$PbTiO_3$. J Alloys Compd 709:16–23
40. Seshadri R, Nicola A (2001) Visualizing the role of Bi 6s "lone pairs" in the off-center distortion in ferromagnetic $BiMnO_3$. Chem Mater 13:2892–2899

41. Singh A, Chatterjee R (2012) Multiferroic properties of La-rich $BiFeO_3$–$PbTiO_3$ solid solutions. Ferroelectrics 433:180–189
42. Freitas VF, Santos IA, Botero E, Fraygola BM, Garcia D, Eiras JA (2011) Piezoelectric characterization of (0.6)$BiFeO_3$–(0.4)$PbTiO_3$ multiferroic ceramics. J Am Ceram Soc 94:754–758
43. Zalesskii AV, Frolov AA, Khimich TA, Bush AA (2003) Composition-induced transition of spin-modulated structure into a uniform antiferromagnetic state in a $Bi_{1-x}La_xFeO_3$ system studied using ^{57}Fe NMR. Phys Solid State 45:141–1457
44. Ruette B, Zvyagin S, Pyatakov AP, Bush A, Li JF, Belotelov Zvezdin AK, Viehland D (2004) Magnetic-field-induced phase transition in $BiFeO_3$ observed by high-field electron spin resonance: cycloidal to homogeneous spin order. Phys Rev B 69:064114-7
45. Mathe VL, Patankar KK, Patil RN, Lokhande CD (2004) Synthesis and dielectric properties of $Bi_{1-x}Nd_xFeO_3$ perovskites. J Magn Magn Mat 270:380–388
46. Pradhan SK, Das SN, Bhuyan S, Behera C, Padhee R, Choudhary RNP (2016) Structural, dielectric and impedance characteristics of lanthanum-modified $BiFeO_3$–$PbTiO_3$ electronic system. Appl Phys A 122:604
47. Zhou Q, Zhou C, Yang H, Chen G, Li W, Wang H (2012) Dielectric, ferroelectric, and piezoelectric properties of $Bi(Ni_{1/2}Ti_{1/2})O_3$-modified $BiFeO_3$–$BaTiO_3$ ceramics with high curie temperature. J Am Ceram Soc 95:3889
48. Chen X, Wang Y, Yang Y, Yuan G, Yin J, Liu Z (2012) Structure, ferroelectricity and piezoelectricity evolutions of $Bi_{1-x}Sm_xFeO_3$ at various temperatures. Solid State Commun 152:497
49. Comyn TP, McBride SP, Bell AJ (2004) Processing and electrical properties of $BiFeO_3$–$PbTiO_3$ ceramics. Mater Lett 58:3844–3846
50. Jiang B, Li X, Zhang H, Sun W, Liu J, Hu G (2012) Large and stable piezoelectric response in $Bi_{0.97}Nd_{0.03}FeO_3$ thin film. Appl Phys Lett 100:172904